SELF-RECOVERING MULTIRATE EQUALIZERS USING REDUNDANT FILTERBANK PRECODERS

Anna Scaglione[1], *Georgios B. Giannakis*[2], *Sergio Barbarossa*[1]

[1] Univ. of Rome "La Sapienza", Infocom Dept., ITALY; {sergio,annas}@infocom.ing.uniroma1.it
[2]Dept. of Elec. Engr., Univ. of Virginia, Charlottesville, VA 22903, USA; georgios@virginia.edu

ABSTRACT

Transmitter redundancy introduced using FIR filterbank precoders offers a unifying framework for single- and multi-user transmissions. With minimal rate reduction, FIR filterbank transmitters with trailing zeros allow for perfect (in the absence of noise) equalization of FIR channels with FIR zero-forcing equalizer filterbanks, *irrespective* of the input color and the channel zero locations. Exploiting *input diversity*, blind channel estimators, block synchronizers, and direct self-recovering equalizing filterbanks are derived in this paper. The resulting algorithms are computationally simple, require small data sizes, can be implemented online, and remain consistent (after appropriate modifications) even at low SNR colored noise. Simulations illustrate applications to multi-carrier modulations through channels with deep fades, and superior performance relative to CMA and existing output diversity techniques relying on multiple antennas and fractional sampling.

1. INTRODUCTION

Redundancy at the transmitter builds *input diversity* in digital communication systems and is well motivated for designing error correcting codes (e.g., [1]). But recently, input diversity has been exploited also for ISI suppression using precoders operating in the complex (as opposed to Galois) field, [4, 6], [8, 9, 10], [12]). Different precoding schemes are possible. Multiplying the inaccessible input by a known periodic sequence offers non-redundant precoding without decreasing the information rate, although the constellation's modulus is affected and equalization of FIR channels with FIR equalizers is impossible [9]. On the other hand, repeating input symbols as in [10], leads to FIR equalizers but reduces information rate by half. Combining desired features, filterbank precoders and blind equalizers were proposed in [4], to minimize the rate reduction, and obviate channel zero restrictions imposed by spatio-temporal *output diversity* methods that rely upon fractional sampling and/or multiple-antenna reception [11], [13]. However, identifiability in [4] was established only for white inputs and linear equation or subspace algorithms were developed for simple precoders (see also [6]). In a deterministic multirate framework, filterbanks for non-blind channel equalization were also proposed in [12] under restrictions on the channel zeros.

Redundant filterbank precoders offer a unifying discrete-time model which encompasses a wide range of digital modulation and coding schemes [8]. Those include: periodic and line codes, orthogonal frequency-division multiplexing (OFDM) and discrete multitone (DMT) [2], fractional sampling [11], (de-)interleaving, as well as multi-user transmissions such as TDMA, FDMA, CDMA, and the most recent discrete wavelet multiple access (DWMA) schemes [7]. Redundant precoding brings input diversity similar to that available with training sequences which have been exploited recently in a semi-blind channel estimation framework [5]. However, filterbank precoders spread the training bits across all the blocks over which the channel may be changing.

Motivated by the generality and importance of filterbank precoders, this paper builds upon [4] and [8] and derives blind channel estimation and block synchronization algorithms, as well as direct blind FIR equalizing filterbanks that allow for deterministic and (white or colored) random inputs (important for coded transmissions), without imposing restrictions on channel zeros (Section 3). General precoders equipped with trailing zeros (TZ) offer computationally simple algorithms and lead to zero-forcing (ZF) or minimum mean-square error (MMSE) equalizing filterbanks that accept also adaptive implementations. Exciting options become available for blind equalization in OFDM – a transmission standard for Digital Audio Broadcasting [2], which is known to suffer from deep channel fades (see also [3]). Consistency analysis and modifications needed at low SNR environments are given also in Section 3 while simulations and comparisons with FS and CMA alternatives are described in Section 4.

2. PRELIMINARIES

Consider the discrete-time multirate transmitter model of the baseband communication system in Fig. 1. Downsamplers and upsamplers perform blocking (i.e., multiplexing) and un-blocking (de-multiplexing) operations. With $P > M$, the ratio $(P-M)/P$ represents the amount of redundancy introduced. Transmit filters $\{f_m(n)\}_{m=0}^{M-1}$ are FIR of maximum order $P-1$, while the Lth order channel $\{h(l)\}_{l=0}^{L}$ captures multipath effects and timing ambiguities as delay factors. The input to the upsampler of the mth branch is $s_m(n) := s(nM+m)$. It represents the m-th symbol in the n-th block of M symbols, while in the multi-user case it stands for the mth user's bits. With the insertion of $P-1$ zeros, the corresponding upsampler's output is: $u_m(n) = \sum_i s_m(i)\delta(n-iP)$, where $\delta(n)$ denotes Kronecker's delta. We will assume Nyquist signaling pulses; hence, their effect disappears in discrete-time and the transmitted sequence is: $u(n) = \sum_{m=0}^{M-1} u_m(n) = \sum_i \sum_{m=0}^{M-1} s_m(i) f_m(n-iP)$. To obtain a block data model, we define $M \times 1$ vector $\mathbf{s}(n) := (s_0(nM)s_1(nM)\cdots s_{M-1}(nM))^T$, $P \times 1$ vectors $\mathbf{x}(n) := (x(nP)x(nP+1)\cdots x(nP+P-1))^T$, $\mathbf{f}_m := (f_m(0)\cdots f_m(M-1)0\cdots 0)^T$, $P \times M$ precoder matrix $\mathbf{F} := (\mathbf{f}_0 \cdots \mathbf{f}_{M-1})$, and $P \times P$ Toeplitz lower triangular matrix $\mathbf{H}_0$ with first column $(h(0)\cdots h(L)0\cdots 0)^T$. We assume:

(a0) Channel $h(l)$ is Lth order FIR with $h(0), h(L) \neq 0$.

(a1) For a given L, the pair (P, M) is chosen to satisfy $P > M > L$ and $P = M + L$.

Based on (a0), (a1), the received block data model is [8]:

$$\mathbf{y}(n) = \mathbf{x}(n) + \mathbf{v}(n) = \mathbf{H}_0\mathbf{F}\mathbf{s}(n) + \mathbf{v}(n)\,. \quad (1)$$

Furthermore, we will assume here that:

(a2) Precoder filters have L trailing zeros; i.e., $\{f_m(n)\}_{n=M}^{P} = 0$, $\forall\, m \in [0, M-1]$, and are linearly independent; i.e., $rank(\mathbf{F}) = M$, which guarantees one-to-one mapping and thus recovery of $s(n)$ from the coded symbols $u(n)$.

(a3) There exists an $N \geq P$, such that the $M \times N$ matrix $\mathbf{S} := (\mathbf{s}(0)\cdots\mathbf{s}(N-1))$ has full rank M. With white inputs, $\mathbf{SS}^H$ tends (as N increases) to the input correlation matrix $\mathbf{R}_{ss}$. But (a3) will be satisfied even for colored (e.g., coded) inputs provided that their spectra are non-zero for at least M frequencies (modes).

With moderate or large number of filters M in the precoder, the maximum likelihood (ML) receiver implemented with Viterbi's algorithm has prohibitively large complexity which motivates looking for linear (and preferably low order FIR) equalizing filterbanks. ZF solutions offer (almost) perfect symbol recovery in (high SNR) noise-free environments and their performance in terms of error probability is easily computable. Sufficient conditions for their existence and uniqueness were derived in [8]:

Theorem 1 *Given* $\mathbf{F}$ *and* $\mathbf{H}_0$*, there exists under (a0)-(a2) a zero order* $M \times P$ *equalizing filterbank such that* $\mathbf{Gx}(n) = \mathbf{s}(n)$*. Minimum norm ZF filterbank is unique and is given by:* $\mathbf{G}_{zf} = (\mathbf{H}_0\mathbf{F})^\dagger$*, where* $\dagger$ *denotes pseudo-inverse.* □

Note that Thm. 1 poses no constraints on the channel zeros. In contrast, FIR-ZF equalizers in [11, 13, 10, 12] do not exist for certain configurations of channel zeros on the unit circle, and more important, performance degrades even when channels have zeros close to those non-invertible configurations. If an upper bound $\bar{L} \geq L$ is only available on the channel order, Thm. 1 holds true with $\bar{L}$ replacing L in (a1). Because for a fixed bandwidth the information rate depends upon the ratio M/P, we note that under (a1), the rate reduction can be made arbitrarily small by selecting M (and thus P) sufficiently large.

In the presence of noise, a vector MMSE (or Wiener) equalizer can be derived by minimizing $E\{tr[\mathbf{Gy}(n)-\mathbf{s}(n)][\mathbf{Gy}(n)-\mathbf{s}(n)]^H\}$. It is given by [8]:

$$\mathbf{G}_{mmse} = \mathbf{R}_{ss}\mathbf{F}^H\mathbf{H}_0^H(\mathbf{R}_{vv} + \mathbf{H}_0\mathbf{F}\mathbf{R}_{ss}\mathbf{F}^H\mathbf{H}_0^H)^{-1}\,. \quad (2)$$

Note that both $\mathbf{G}_{zf}$ and $\mathbf{G}_{mmse}$ require channel estimates which we derive next based on the received data only.

3. BLIND SYMBOL RECOVERY

Blind channel estimation is well motivated for wireless environments where the multipath channel changes rapidly as the mobile communicators move. Self-recovering equalization schemes are thus important to avoid frequent retraining and thus increase bandwidth efficiency.

3.1. Blind Channel Estimation

Under (a2), $\mathbf{x}(n) = \mathbf{H}_0\mathbf{Fs}(n) = \tilde{\mathbf{H}}_0\tilde{\mathbf{F}}\mathbf{s}(n)$, where $\tilde{\mathbf{H}}_0$ is formed by the first M columns of $\mathbf{H}_0$. Collecting N data vectors $\{\mathbf{x}(n)\}_{n=0}^{N-1}$ in a matrix, we arrive at:

$$\mathbf{X}_N \;:=\; (\mathbf{x}(0)\cdots\mathbf{x}(N-1)) \;=\; \tilde{\mathbf{H}}_0\,\tilde{\mathbf{F}}\,\mathbf{S}\,, \quad (3)$$

where $\mathbf{S}$ is defined as in (a3). Because of (a0), $h(0) \neq 0$, and thus $rank(\tilde{\mathbf{H}}_0) = M$, which along with (a2) and (a3) imply that $rank(\mathbf{X}_N) = M$. Therefore, the nullity of the matrix $\mathbf{X}_N\mathbf{X}_N^H$ is: $\nu(\mathbf{X}_N\mathbf{X}_N^H) = P - M = L$, and the eigen-decomposition

$$\mathbf{X}_N\mathbf{X}_N^H \;=\; (\bar{\mathbf{U}}\,\tilde{\mathbf{U}})\begin{pmatrix}\mathbf{\Sigma}_{M\times M} & \mathbf{0}_{M\times L}\\ \mathbf{0}_{L\times M} & \mathbf{0}_{L\times L}\end{pmatrix}\begin{pmatrix}\bar{\mathbf{U}}^H\\ \tilde{\mathbf{U}}^H\end{pmatrix}\,, \quad (4)$$

yields the $P \times L$ matrix $\tilde{\mathbf{U}}$ whose columns span the nullspace $\mathcal{N}(\mathbf{X}_N)$. Since $\tilde{\mathbf{F}}\mathbf{S}$ in (3) is full rank, $\mathcal{R}(\mathbf{X}_N) = \mathcal{R}(\mathbf{H}_0)$, where $\mathcal{R}$ stands for range space. But since $\mathcal{R}(\mathbf{X}_N)$ is orthogonal to $\mathcal{N}(\mathbf{X}_N)$, it follows that:

$$\tilde{\mathbf{U}}^H\,\tilde{\mathbf{H}}_0 \;=\; \mathbf{0} \;\Rightarrow\; \tilde{\mathbf{u}}_l^H\,\boldsymbol{\mathcal{T}}(\mathbf{h}) \;=\; \mathbf{0}^H\,, \quad l = 1,\ldots,L \quad (5)$$

where $\tilde{\mathbf{u}}_l$ denotes the lth column of $\tilde{\mathbf{U}}$ and $\boldsymbol{\mathcal{T}}(\mathbf{h})$ is lower triangular Toeplitz with first column $(h(0)\cdots h(L)0\cdots 0)^T$. But vector multiplication with a Toeplitz matrix denotes convolution which is commutative and thus (5) can be written as:

$$\mathbf{h}^H\,\mathcal{U} \;:=\; \mathbf{h}^H\,(\mathcal{U}_1\cdots\mathcal{U}_L) \;=\; \mathbf{0}^H\,, \quad (6)$$

where each $\mathcal{U}_l$ is an $(L+1)\times M$ Hankel matrix formed by $\tilde{\mathbf{u}}_l$. Our result and corresponding algorithm are summarized in the following:

Theorem 2 *Let (a0)-(a3) hold true. Starting from the data matrix* $\mathbf{X}_N$*, let us form the* $(L+1)\times ML$ *matrix* $\mathcal{U}$ *as in (3)-(6). Channel vector* $\mathbf{h}$ *can then be obtained as the unique (within a scale) null eigen-vector of* $\mathcal{U}$ *in (6).* □

With the channel matrix $\mathbf{H}_0$ available, we can proceed to determine either the ZF equalizer filterbank from Thm. 1, or, the MMSE equalizer from (2). In fact, it is possible to derive MMSE equalizers involving a delayed decision (with or without feedback), or, pursue the computationally complex but optimal ML receiver. Instead, we focus next on direct blind equalizers that do not even require channel estimation as a first step and being linear, they lend themselves naturally to online self-recovering algorithms.

3.2. Direct Blind Equalization

Collect $\{\mathbf{x}(n)\}_{n=0}^{N-1}$ blocks to form the data matrix $\mathbf{X}_N$ as in (3), and define $\mathbf{\Gamma} := \mathbf{H}_0^{-1}$ to arrive at:

$$\mathbf{\Gamma}\,\mathbf{X}_N \;=\; \begin{pmatrix}\tilde{\mathbf{F}}\mathbf{S}(n)\\ \mathbf{0}_{L\times 1}\end{pmatrix}\,. \quad (7)$$

Because the $P \times P$ matrix $\mathbf{H}_0$ is lower triangular Toeplitz, it follows easily (by forming $\mathbf{\Gamma}\mathbf{H}_0 = \mathbf{I}$) that the inverse $\mathbf{\Gamma}$ is also lower triangular Toeplitz. Thus, all the rows $\{\boldsymbol{\gamma}_i^T\}_{i=1}^P$ of $\mathbf{\Gamma}$ can be obtained from the last row $\boldsymbol{\gamma}_P^T$. Relying on (7), we will show how $\boldsymbol{\gamma}_P^T$ can be determined using only the received data matrix $\mathbf{X}_N$ in (3).

Let $\mathbf{J}$ denote a $P \times P$ shift matrix having all ones in the first sub-diagonal and all other entries zero. Using $\mathbf{J}$, the rows of $\mathbf{\Gamma}$ can be successively related: $\boldsymbol{\gamma}_i^T = \boldsymbol{\gamma}_{i+1}^T\mathbf{J}$ $\boldsymbol{\gamma}_{i+2}^T\mathbf{J}^2 = \cdots = \boldsymbol{\gamma}_P^T\mathbf{J}^{P-i}$, which implies that

$$\boldsymbol{\gamma}_P^T\mathbf{J}^{P-i}\,\mathbf{X}_N \;=\; \boldsymbol{\gamma}_i^T\,\mathbf{X}_N\,, \quad i = 1,\ldots,P\,. \quad (8)$$

But focusing on the last L rows of (7), it follows that for $i = P, P-1, \ldots, P-L+1$ we have $\boldsymbol{\gamma}_i^T\mathbf{X}_N = \mathbf{0}^T$, which after employing (8) leads to

$$\boldsymbol{\gamma}_P^T\,\boldsymbol{\mathcal{X}}_N \;:=\; \boldsymbol{\gamma}_P^T\,\left(\mathbf{X}_N\,\mathbf{J}\mathbf{X}_N\cdots\mathbf{J}^{L-1}\mathbf{X}_N\right) \;=\; \mathbf{0}^T\,. \quad (9)$$

It can be shown that the nullity $\nu(\boldsymbol{\mathcal{X}}_N) = 1$; thus, $\boldsymbol{\gamma}_P^T$ (and hence $\mathbf{\Gamma}$) can be determined from (9). In summary:

Theorem 3 *Let (a0)-(a5) hold true. Then,* $\nu(\boldsymbol{\mathcal{X}}_N) = 1$*, and* $\boldsymbol{\gamma}_P^T$ *can be identified from (9) as the unique (within a scalar ambiguity) null eigen-vector of* $\boldsymbol{\mathcal{X}}_N\boldsymbol{\mathcal{X}}_N^H$*. With* $\boldsymbol{\gamma}_P^T$ *as the* P*th row, the lower triangular Toeplitz matrix* $\mathbf{\Gamma}$ *can be built and used in Thm. 1 to obtain* $\mathbf{G}_{zf}$ *directly.* □

The equalizer implied by Thm. 3 neither invokes any restrictions on the channel zeros nor it relies on any statistical input assumptions (e.g., whiteness as in [4]). It thus recovers the input exactly in the absence of noise. Because only $N \geq P$ data blocks are required in $\mathbf{X}_N$, and each $\mathbf{x}(n)$ is $P \times 1$, the minimum number of symbols required is P^2.

Remark: With $f_m(n) = \exp(j2\pi mn/M)$, the filterbank precoder of Fig. 1, reduces to the digital OFDM transmitter [2]. Under (a2), the trailing zeros TZ-OFDM (detailed in [8]) can be equalized blindly even when $h(n)$ has unit circle zeros located at $2\pi m/M$ – a case where deep fades deteriorate performance of conventional OFDM (see also [3]).

3.3. Direct Blind Synchronization

Eq. (1) assumes that block synchronization has been accomplished. Although techniques relying on training data are available, it is possible to achieve block synchronization blindly – a task complementing our blind equalizer nicely (see also [10] for a statistical method). A deterministic blind approach is proposed herein after observing that matrix $\boldsymbol{\mathcal{X}}_N$ in (9) becomes full rank when the receiver is not block synchronous. If blocks at the receiver are off by $d = t_0$ samples and one forms $\boldsymbol{\mathcal{X}}_N^{(d)}$ matrices for each possible shift d, then t_0 can be found as:

$$t_0 = \text{argmin}_d \, \lambda_{min}(\boldsymbol{\mathcal{X}}_N^{(d)} \boldsymbol{\mathcal{X}}_N^{(d)H}) , \quad (10)$$

where $\lambda_{min}(\boldsymbol{\mathcal{X}}_N^{(d)} \boldsymbol{\mathcal{X}}_N^{(d)H})$ denotes the minimum eigenvalue. In the noise-free case, we have $\lambda_{min}(\boldsymbol{\mathcal{X}}_N^{(d)} \boldsymbol{\mathcal{X}}_N^{(d)H}) = 0$ according to Thm. 3, and $\lambda_{min}(\boldsymbol{\mathcal{X}}_N^{(d)} \boldsymbol{\mathcal{X}}_N^{(d)H}) > 0$ for $d \neq t_0$.

3.4. Noisy Case – Consistency

When stationary additive noise $v(n)$ is present, our data covariance matrix $\mathbf{R}_{yy} := E\{\mathbf{y}(n)\mathbf{y}^H(n)\}$ is given by

$$\mathbf{R}_{yy} = \mathbf{R}_{xx} + \mathbf{R}_{vv} = \tilde{\mathbf{H}}_0 \tilde{\mathbf{F}} \mathbf{R}_{ss} \tilde{\mathbf{F}}^H \tilde{\mathbf{H}}_0 + \mathbf{R}_{vv} . \quad (11)$$

Similar to (a3), we assume that:

(a3') The $M \times M$ covariance matrix $\mathbf{R}_{ss}$ is full rank;

Based on (a2) and (a3') we have $rank(\tilde{\mathbf{F}}\mathbf{R}_{ss}\tilde{\mathbf{F}}^H) = M$, whereas (a0) implies that $rank(\tilde{\mathbf{H}}_0) = M$. Hence, $rank(\mathbf{R}_{xx}) = M$, and $\nu(\mathbf{R}_{xx}) = P - M = L$, which yields an L-dimensional noise subspace $\tilde{\mathbf{U}}_x$ in the eigendecomposition $\mathbf{R}_{xx} = \mathbf{U}_x \boldsymbol{\Sigma}_x \mathbf{U}_x^H$, where $\mathbf{U}_x := (\bar{\mathbf{U}}_x \, \tilde{\mathbf{U}}_x)$. Arguing exactly as in (4), (5), we arrive at the orthogonality condition: $\tilde{\mathbf{U}}_x^H \, \tilde{\mathbf{H}}_0 = \mathbf{0}$. Consider now the eigendecomposition $\mathbf{R}_{vv} = \sigma_v^2 \mathbf{U}_v \mathbf{U}_v^H$ and based on $\mathbf{U}_v$, eigendecompose $\mathbf{U}_v^{-1} \mathbf{R}_{yy} \mathbf{U}_v^{-H}$ as:

$$\begin{aligned} \mathbf{U}_v^{-1} \mathbf{R}_{yy} \mathbf{U}_v^{-H} &= \mathbf{U}_v^{-1} \mathbf{U}_x (\boldsymbol{\Sigma}_x + \sigma_v^2 \mathbf{I}) \mathbf{U}_v^H \mathbf{U}_v^{-H} \quad (12) \\ &:= \mathbf{U}_y \boldsymbol{\Sigma}_y \mathbf{U}_y^{-1} = (\bar{\mathbf{U}}_y \tilde{\mathbf{U}}_y) \, \boldsymbol{\Sigma}_y \begin{pmatrix} \bar{\mathbf{U}}_y^H \\ \tilde{\mathbf{U}}_y^H \end{pmatrix} \end{aligned}$$

from which it follows easily that $\tilde{\mathbf{U}}_y = \mathbf{U}_v^{-1} \tilde{\mathbf{U}}_x$. Substituting the latter to our orthogonality condition, we find: $\tilde{\mathbf{U}}_y^H \, \mathbf{U}_v^H \, \tilde{\mathbf{H}}_0 = \mathbf{0}$, which implies that our blind channel identification algorithm applies even in the noisy case provided that $\mathbf{R}_{vv}$ (and hence $\mathbf{U}_v$) are known. Note also that knowledge of σ_v^2 is not necessary if $\mathbf{v}(n)$ is white.

In practice, sample averages replace ensemble correlation matrices and consistency of our algorithm is guaranteed because $\mathbf{y}(n)$ in (1) is mixing (input $s(n)$ has finite moments and $h(n)$ has finite memory); thus,

$$\hat{\mathbf{R}}_{yy}^{(N)} := \frac{1}{N} \sum_{n=0}^{N-1} \mathbf{y}(n)\mathbf{y}^H(n) \xrightarrow{\text{m.s.s}} \mathbf{R}_{yy} , \quad \text{as} \quad N \to \infty ,$$

where m.s.s. stands for mean-square convergence. Because $\tilde{\mathbf{U}}_y$ is continous function of $\mathbf{R}_{yy}$, it follows that the channel estimator will be consistent.

The same argument establishes consistency of our deterministic approach in Section 3.1 when $v(n)$ is white, if one observes that

$$\hat{\mathbf{R}}_{yy}^{(N)} = \frac{1}{N} \mathbf{Y}_N \, \mathbf{Y}_N^H , \quad (13)$$

where $\mathbf{Y}_N$ is formed exactly as $\mathbf{X}_N$ in (3) but with noisy data, and with subscript N denoting the number of blocks.

Turning now back to the direct equalizer of Section 3.3, we find that:

$$\boldsymbol{\Gamma} \, \mathbf{R}_{xx} = \begin{pmatrix} \tilde{\mathbf{F}} \mathbf{R}_{ss} \tilde{\mathbf{F}}^H \tilde{\mathbf{H}}_0^H \\ \mathbf{0}_{L \times P} \end{pmatrix} \Rightarrow \bar{\boldsymbol{\gamma}}_P^T \, \mathbf{R}_{xx} = \mathbf{0}^T , \quad (14)$$

and arguing as in (8) we infer that $\boldsymbol{\gamma}_P^T \mathbf{J}^l \mathbf{R}_{xx} = \mathbf{0}^T$, which implies that $\boldsymbol{\gamma}_P^T \mathbf{J}^l \mathbf{R}_{xx} (\mathbf{J}^l)^T = \mathbf{0}^T$, for $l = 0, 1, \ldots, L-1$. Hence,

$$\boldsymbol{\gamma}_P^T \, \boldsymbol{\mathcal{R}}_{xx} = \mathbf{0}^T , \quad \boldsymbol{\mathcal{R}}_{xx} := \sum_{l=0}^{L-1} \mathbf{J}^l \mathbf{R}_{xx} (\mathbf{J}^l)^T . \quad (15)$$

where $\boldsymbol{\mathcal{R}}_{xx}$ can be shown to have nullity $\nu(\boldsymbol{\mathcal{R}}_{xx}) = 1$. Thus, if noise were not present, $\boldsymbol{\gamma}_P$ (and hence $\boldsymbol{\Gamma}$) could be obtained (within a scale) as the null eigen-vector of $\boldsymbol{\mathcal{R}}_{xx}$. In the noisy case we define $\boldsymbol{\mathcal{R}}_{yy}$ ($\boldsymbol{\mathcal{R}}_{vv}$) as $\boldsymbol{\mathcal{R}}_{xx}$ in (15) with $\mathbf{R}_{yy}$ ($\mathbf{R}_{vv}$) replacing $\mathbf{R}_{xx}$. Eigen-decomposing $\boldsymbol{\mathcal{R}}_{vv} = \sigma_v^2 \mathcal{U}_v \mathcal{U}_v^H$, and using (11) we can write

$$\begin{aligned} \mathcal{U}_v^{-1} \boldsymbol{\mathcal{R}}_{yy} \mathcal{U}_v^H &= \mathcal{U}_v^{-1} \boldsymbol{\mathcal{R}}_{xx} \mathcal{U}_v^H + \sigma_v^2 \mathbf{I}_{P \times P} \\ &= \mathcal{U}(\boldsymbol{\Lambda} + \sigma_v^2 \mathbf{I}) \mathcal{U}^H . \quad (16) \end{aligned}$$

Next, we define $\bar{\boldsymbol{\gamma}}_P^T := \boldsymbol{\gamma}_P^T \, \mathcal{U}_v$, and use (15) to arrive at $\bar{\boldsymbol{\gamma}}_P^T \mathcal{U}_v^{-1} \boldsymbol{\mathcal{R}}_{xx} = \mathbf{0}^T$, which implies that $\bar{\boldsymbol{\gamma}}_P^T \mathcal{U}_v^{-1} \boldsymbol{\mathcal{R}}_{xx} \mathcal{U}_v^{-H} = \mathbf{0}^T$. The latter along with (16) yields

$$\bar{\boldsymbol{\gamma}}_P^T \, \mathcal{U}_v^{-1} \boldsymbol{\mathcal{R}}_{yy} \mathcal{U}_v^H = \sigma_v^2 \, \bar{\boldsymbol{\gamma}}_P^T , \quad (17)$$

which shows that $\bar{\boldsymbol{\gamma}}_P^T$ is the eigen-vector of $\mathcal{U}_v^{-1} \boldsymbol{\mathcal{R}}_{xx} \mathcal{U}_v^{-H}$ corresponding to the minimum eigenvalue σ_v^2. Based on $\bar{\boldsymbol{\gamma}}_P^T$ we can find $\boldsymbol{\gamma}_P^T = \bar{\boldsymbol{\gamma}}_P^T \mathcal{U}_v^{-1}$ and thus the direct equalizer $\boldsymbol{\Gamma}$ relying only on the noisy covariance matrix $\boldsymbol{\mathcal{R}}_{yy}$ and knowledge of the noise covariance $\boldsymbol{\mathcal{R}}_{vv}$.

If $v(n)$ is white, then $\boldsymbol{\mathcal{R}}_{vv} := \sigma_v^2 \sum_{l=0}^{L-1} \mathbf{J}^l (\mathbf{J}^l)^T = \sigma_v^2 \, diag(1 \, 2 \cdots L \cdots L)$, and its spectral factor in (17) is:

$$\mathcal{U}_v := diag(1 \, \sqrt{2} \cdots \sqrt{L} \cdots \sqrt{L}) . \quad (18)$$

With sample averages only available, consistency of our direct equalizer estimator follows easily.

The same argument establishes consistency of our deterministic method in Section 3.2 if we recall the definition of $\mathbf{Y}_N$ in (13) and note that

$$\hat{\boldsymbol{\mathcal{R}}}_{yy}^{(N)} = \frac{1}{N} \mathcal{Y}_N \, \mathcal{Y}_N^H , \quad \mathcal{Y}_N := (\mathbf{Y}_N \, \mathbf{J}\mathbf{Y}_N \cdots \mathbf{J}^{L-1}\mathbf{Y}_N) . \quad (19)$$

When the SNR is high, the deterministic solution should be preferred and the minimal number of blocks $N = P$ should be used for computational simplicity. However, at low SNR, N should be chosen large enough to obtain reliable estimates $\hat{\boldsymbol{\mathcal{R}}}_{yy}^{(N)}$.

4. SIMULATIONS – COMPARISONS

Example 1 (Blind Synchronization): We implemented the system in Fig. 1 with $(P, M, L) = (19, 16, 3)$ and channel with zeros at: $0.9, j, -j$ ($SNR = 10dB$). Matrix $\mathcal{Y}_N^{(d)}$ with $N = 19^2$ was formed as in (19), collecting in a matrix $\mathbf{Y}^{(d)}$ the vectors $\mathbf{y}^{(d)}(n) = (y(nP+d), \cdots, y(nP+d+P-1))$ for different delays $d \in [0, 8]$, and the minimum eigenvalue of $\mathcal{Y}_N^{(d)} \mathcal{Y}_N^{(d)H}$ was evaluated according to (10) for each d and plotted in Fig. 2 (sample mean with solid and st. deviation bounds with dashed computed based on 100 Monte Carlo runs). The true delay was $t_0 = 0$ and the curves in Fig. 2 indicate clearly a minimum at $d = 0$, illustrating that it is possible to estimate the correct time offset as in (10).

Example 2 (Blind Channel Estimation vs [13]): Fig. 3 shows the root-mean square error (RMSE) of the blind channel estimate of our approach (solid line) and the deterministic approach in [13] (dashed line), based on the channel simulated in [13, Table II]. For both cases 100 data samples were used for blind channel estimation. The advantage of this paper's approach is evident, although we used only one of the four channels used in [13]. This illustrates that introducing redundancy at the transmitter improves performance, relative to methods that rely on output redundancy, while at the same time receiver complexity is reduced.

Example 3 (Direct Blind Equalizer – CMA comparison): We simulated $N = 19$ blocks of 8-PSK symbols, each block with $P = 19$ ($M = 16$ information symbols and $L = 3$ TZs). The 3rd-order channel had zeros at: $0.9, j, -j$, and the SNR at the receiver was fixed at 13 dB. With this relatively low-SNR, we implemented the deterministic direct equalizer approach summarized in Thm. 3, using the minimal number of samples $P^2 = 361$. To compare with Constant Modulus Algorithm (CMA), Fig. 4 shows the scattering diagram obtained in the following cases: (a)without equalization, (b)with the ZF equalizer of Thm.1, (c)with the MMSE equalizer of (2), and (d)with the CMA. For the CMA, we used a 30-tap equalizer and the adaptation rule has run over $N = 10,000$ samples at $SNR = \infty$.

REFERENCES

[1] S. Benedetto, E. Biglieri and V. Castellani, *Digital Transmission Theory,* Prentice-Hall Inc., 1987.

[2] L. J. Cimini, "Analysis and simulation of a digital mobile channel using orthogonal frequency division multiple access," *IEEE Trans. on Com.*, pp. 665-675, 1995.

[3] M. de Courville, P. Duhamel, P. Madec, and J. Palicot, "A least mean-squares blind equalization technique for OFDM systems," *Annal. des Telecom.*, pp. 4-11, 1997.

[4] G. B. Giannakis, "Filterbanks for blind channel identification and equalization," *IEEE Signal Processing Letters*, pp. 184-187, June 1997.

[5] A. Gorokhov and P. Loubaton, "Semi-blind second-order identification of convolutive channels," *Proc. of Intl. Conf. on ASSP,* vol. V, Munich, Germany, 1997.

[6] S. D. Halford and G. B. Giannakis, "Blind Equalization of TDMA Wireless Channels Exploiting Guard Time Induced Cyclostationarity," *Proc. of 1st IEEE Signal Proc. Wrksp. on Wireless Com.,* pp. 117-120, Paris, France, April 16-18, 1997.

[7] S. D. Sandberg and M.A.Tzannes, "Overlapped discrete multitone modulation for high speed copper wire communications" *IEEE J. on Sel. Areas in Com.*, pp. 1571-1585, 1995.

[8] A. Scaglione, G. B. Giannakis, and S. Barbarossa, "Redundant Filterbank Precoders and Equalizers, Parts I and II," *IEEE Trans. on Signal Processing*, 1997 (submitted); see also *Proc. of 35th Annual Allerton Conf.*, Monticello, IL, Sept. 1997.

[9] E. Serpedin and G. B. Giannakis, "Blind channel identification and equalization with modulation induced cyclostationarity," *Proc. CISS*, pp. 792-797, vol. 2, Baltimore MD, March 1997.

[10] M. K. Tsatsanis and G. B. Giannakis, "Transmitter Induced Cyclostationarity for Blind Channel Equalization," *IEEE Transactions on Signal Processing,* pp. 1785-1794, July 1997.

[11] L. Tong, G. Xu, T. Kailath, "Blind identification and equalization based on second order statistics: A time domain approach", *IEEE Trans. on IT*, pp.340-349, 1994.

[12] X.-G. Xia, "New precoding for ISI cancellation using nonmaximally decimated multirate filterbanks with ideal FIR equalizers," *IEEE Trans. on SP*, pp. 2431-2441, Oct. 1997.

[13] G. Xu, H. Liu, L.Tong, T. Kailath, "A Least-Square Approach to Blind Channel Identification", *IEEE Trans. on SP*, pp.2982-2993, Dec. 1995.

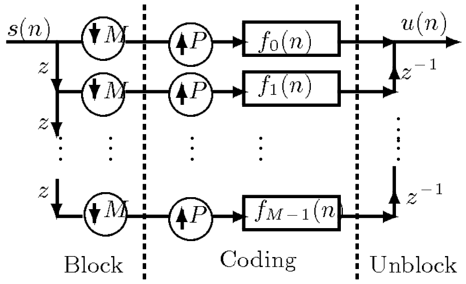

Figure 1. Redundant Filterbank Precoder

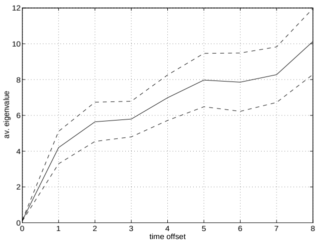

Figure 2. Blind Synchronization via (10).

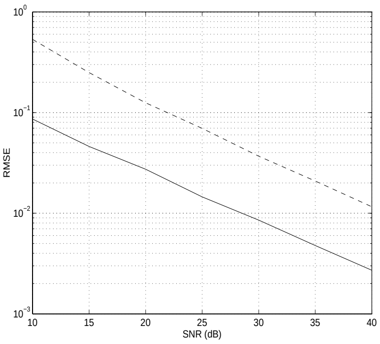

Figure 3. Root-mean square error of the blind estimation.

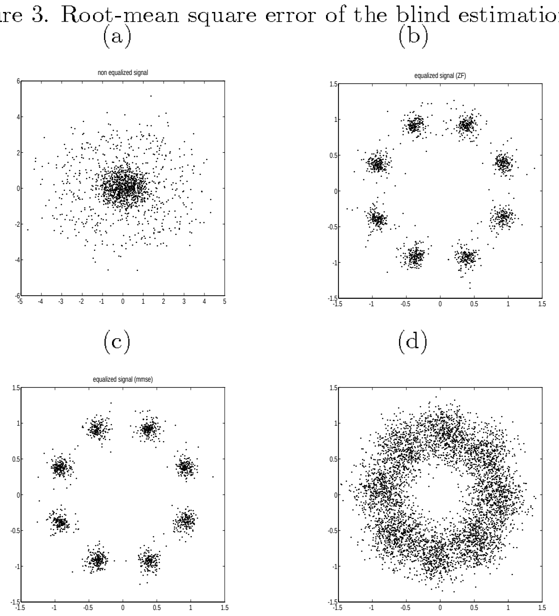

Figure 4. (a)before equalization; (b)after direct ZF equalization; (b)MMSE, $SNR = 13dB$; (c)CMA, $SNR = \infty$.